Open loop control on large stroke MEMS deformable mirrors

Alioune Diouf [1], Thomas G. Bifano [1], Andrew P. Legendre [1], Yang Lu [1], Jason B. Stewart [2]

[1]Boston University Photonics Center, 8 Saint Mary's Street, Brookline, MA 02446, USA

[2]Boston Micromachines Corporation, 30 Spinelli Place, Cambridge, MA 02138

Abstract

Improvements for open-loop control of MEMS deformable mirror for large-amplitude wavefront control are presented. The improvements presented here relate to measurement filtering, characterization methods, and controlling the true, non-differential shape of the mirror. These improvements have led to increased accuracy over a wider variety of deflection profiles including flattening the mirror and Zernike polynomials.

1. Introduction

This work is based on the open-loop control of a MEMS deformable mirror for large-amplitude wavefront presented by Stewart *et al* [1]. Here, we present enhancements of the previous open-loop algorithm by improving the calibration method, the measurements filtering, the characterization method, and the controlling of true ("non-differential") shapes of the mirrors.

2. Existing Open loop models for MEMS DMs

The open-loop control algorithm is based upon a DM model that consists of two coupled mechanical subsystems: the continuous facesheet and the array of actuators connected to the facesheet via rigid posts.

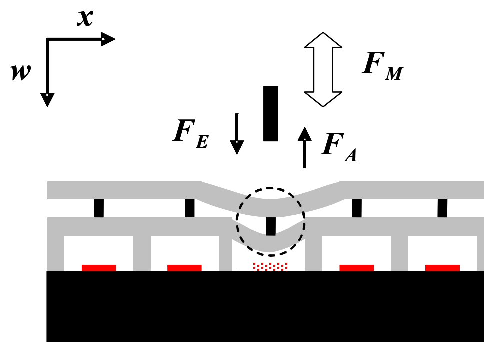

Figure 1: Representation of the DM model. The facesheet is modeled as a thin plate. The electrostatic actuators supporting the facesheet are comprised of a distributed electrostatic force exerting a downward force on a compliant plate clamped along two edges.

MEMS Adaptive Optics IV, edited by Scot S. Olivier, Thomas G. Bifano, Joel A. Kubby, Proc. of SPIE Vol. 7595, 75950D · © 2010 SPIE · CCC code: 0277-786X/10/$18 · doi: 10.1117/12.842489

Downloaded from SPIE Digital Library on 13 Mar 2010 to 24.218.156.200. Terms of Use: http://spiedl.org/terms

We model the out-of-plane deflections using a 4th order partial differential equation (PDE) with nonlinear 2nd order term to account for the effects of the facesheet stretching.

$$\nabla^4 w(x,y) = \frac{q(x,y)}{D} + \frac{6}{h^2}\left[\left(\left(\frac{\partial w(x,y)}{\partial x}\right)^2 \frac{\partial^2 w(x,y)}{\partial x^2}\right) + \left(\left(\frac{\partial w(x,y)}{\partial y}\right)^2 \frac{\partial^2 w(x,y)}{\partial y^2}\right)\right] \quad (1)$$

with deflection w, flexural rigidity D, elastic modulus E, Poisson's ratio ν, surface pressure q, and plate thickness h.

We use the numerical approximation of the biharmonic and Laplacian (4th and 2nd order derivatives) to compute the mirror forces for given mirror deflections. The remaining forces (actuator and electrostatic) are not calculated. Instead, our algorithm proceeds with an empirical characterization of the DM actuators, which consists of applying a variety of arbitrary shapes of known voltages to create a voltage lookup that spans the achievable mirror shapes space. The main drawback of this technique is its susceptibility to noise because of the four numerical differentiations to approximate the biharmonic.

Morzinski *et al* [2] used a similar model for their open-loop control routine. Their routine was able to predict voltages for 500nm amplitude mirror shapes with residual errors of 15nm rms. The model for the facesheet did not account for stretching and the plate equation was solved by treating square geometries as circular:

$$\nabla^4 w_z(r) = \frac{f_P(r)}{D} \quad (2)$$

where f is the force applied at each actuator post. This approximation allowed them to use a free-space Green's function to formulate their open loop control scheme. The authors considered an influence function $K(x,y,x_n,y_n)$ giving deflection (x,y) when a unit load is applied at some point (x_n,y_n). This defines the influence surface for the deflection of the plate at a fixed point (x,y). The circular plate approximation renders it easy to write the influence function (Green's fundamental solution) and arrive at the deflection

$$w(x,y) = \sum_{n=1}^{N.M} f(x_n, y_m) K(x - x_n, y - y_m) \quad (3)$$

where N and M are the number of actuators in the x and y directions ($N = M$ in MEMS DMs considered).

Vogel and Yang [3] introduced a coupled system of non-linear PDEs for the mirror facesheet and actuator. This model did not take into account non-linearity when the displacements are large relative to the plate thickness (stretching) and assumed a parallel plate electrostatic deflection of the actuators. Also by devising a completely analytical solution, the model also failed to capture potential non-negligible actuator post rotational

Downloaded from SPIE Digital Library on 13 Mar 2010 to 24.218.156.200. Terms of Use: http://spiedl.org/terms

compliance (twisting) at the facesheet connection. Vogel et al. recently presented a parameter estimation method based on their prior work. In this work the facesheet stretching is included in the 4th order PDE and the second PDE is eliminated with the actuators treated like linear springs. This approach requires succinct knowledge of the DM to conduct the experiments that will yield accurate parameter estimate.

3. Technical improvements and experiments

The major improvements presented here relate to measurement filtering, characterization methods, and controlling the true, non-differential shape of the mirror. These improvements have led to increased accuracy over a wider variety of deflection profiles including flattening and Zernike polynomials.

Filtering the deflection measurement during calibration is an essential step to reduce the effect of measurement noise and mirror surface defects on the fourth order differentiation that calculates force. Previous work on control of continuous MEMS DMs has filtered out all frequencies outside of the controllable band of the mirror [1]. Using such a restrictive filter leads to loss of information on the bending and stretching behavior of the DM. The forces calculated from an over-filtered measurement spread beyond a single subaperture and can be integrated into the wrong actuator, which results in an inaccurate lookup table. To mitigate the negative effects of filtering, a fourth-order Butterworth filter with a cutoff frequency (250μm) of just below two waves per actuator is used. A Butterworth filter is maximally flat in the passband so that no deflection information is lost and its gradual slope provides some flexibility in choosing a cutoff frequency. The relatively high cutoff frequency used here filters all noise and surface defects, while retaining most information on the bending and stretching of the mirror (2nm RMS error between the filtered and unfiltered data). The calculated forces that result from a higher frequency cutoff are also more concentrated at the post and therefore fit more closely with the analytic model.

Another prominent source of error is the nonuniformity of actuator mechanical behavior that results from tolerances in the manufacturing process [1]. To account for this nonuniformity, a calibration table is created for each individual actuator. Two methods for fast calibration of all actuators have been explored using a “checkerboard” pattern and a grid pattern. Both of these calibration methods are fully scalable, requiring the same number of measurements to characterize a 12x12 actuator array as they would for any larger square array. For the “checkerboard” calibration, the actuators are divided into two groups in a checkerboard pattern. A range of voltages at regular steps is applied to each group independently and information is recorded for all actuators for each measurement. The benefit of this method is that it can be completed in the same number of measurements as a single actuator calibration. The checkerboard method, however, does not characterize high force mirror states and can therefore only be used in a limited number of applications.

Downloaded from SPIE Digital Library on 13 Mar 2010 to 24.218.156.200. Terms of Use: http://spiedl.org/terms

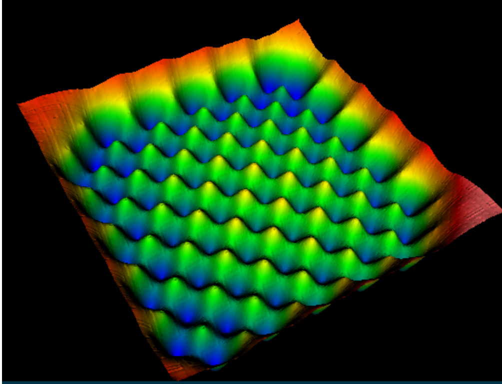

Figure 2: Checkboard pattern used in open loop voltage calibration routine

The grid calibration places every third actuator into the measured group and all the remaining actuators into the unmeasured group. Again, a range of voltages is applied to each group, but data is only collected for the measured group. At the end of a calibration cycle, a new set of actuators is placed into the measurement group and the cycle is repeated until all actuators have been calibrated. This method characterizes the full range of possible mirror states, but requires nine full calibration cycles to complete. This longer calibration time could lead to inaccurate results if the measurement setup is susceptible to drift (2nm rms over 8 hours).

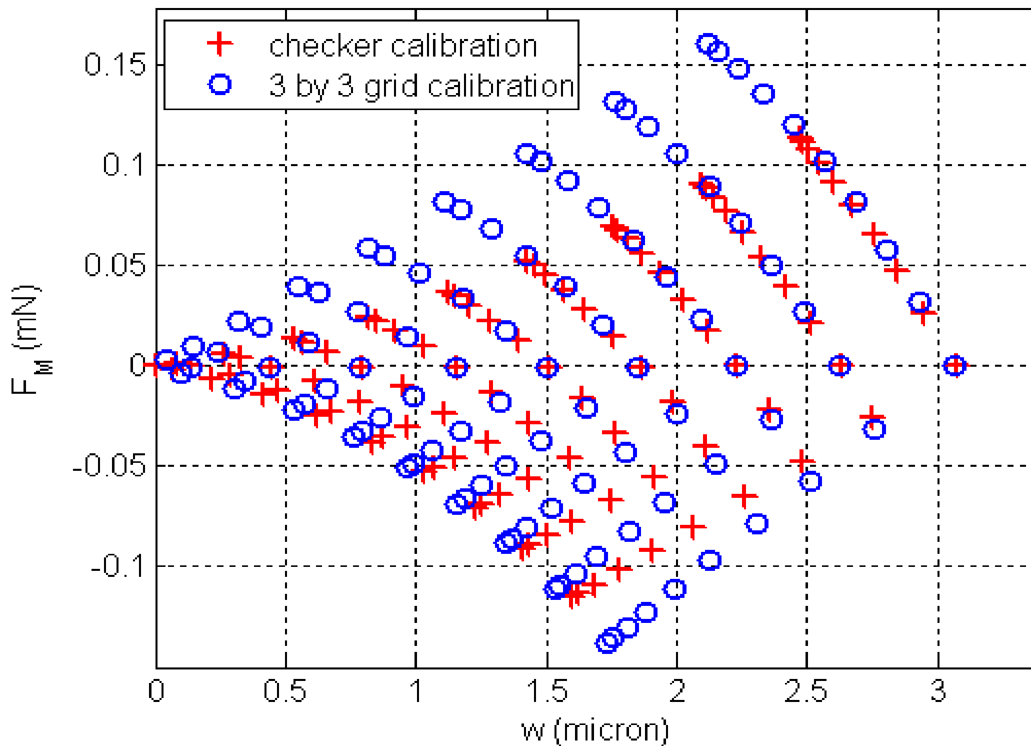

Figure 3: Checkerboard vs. "3 by 3 grid" calibration patterns. The checkerboard calibration (red '+') pattern is completed using the same number of measurements as a single calibration pattern. However it does not span the entire space, missing high forces state.

Downloaded from SPIE Digital Library on 13 Mar 2010 to 24.218.156.200. Terms of Use: http://spiedl.org/terms

One additional measurement of the initial shape of the mirror is added to the calibration to allow control of true, non-differential shapes. This measurement is heavily filtered with a cutoff frequency of a half wave per actuator to get the low-frequency, controllable initial shape. When the filtered shape is sent to the control algorithm, the mirror is flattened to 9 nm within unfiltered RMS error, which is dominated by surface defects. The filtered initial mirror shape is directly added to any desired mirror shape with an additional offset that centers the applied shape within the dynamic range of the mirror. This method effectively runs the open-loop control on a mirror flattened to an offset.

To prepare an arbitrary shape to work with the open-loop model, the edges of the shape must be extended beyond the active area to the edges of the mirror using a smooth profile. This is accomplished by fitting the desired shape to the active mirror aperture and using a plate-model interpolation method to assign appropriate values to the buffer actuators between the active aperture and the edge of the mirror. This method does not alter the control shape and provides an input that is compatible with the open-loop model. Performance of the control algorithm can be further improved by reducing the pupil size to use some of the actuators for an active buffer row, which minimizes errors at the edge of the control aperture.

Relatively simple shapes (i.e. single actuator pokes, piston) resulted in less than 15 nm RMS residual wavefront error at deflections ranging from 0.5 to 3 μm. More complex shapes such as Zernike astigmatism of 1 μm peak-to-valley deflection were applied directly to the MEMS DM resulting in ~9nm RMS error. This error is calculated from a direct measurement compared to the desired shape without subtracting a reference or applying a filter. This error is compared to the difference measurement experiment where we ask the DM to produce a shape that we know a priori the DM can make. The error for this difference measurement compares a previously achieved shape with the open-loop attempt to reproduce that shape and uses the same filter as the calibration. The difference measurement experiment of the same Zernike astigmatism from above results in ~6 nm RMS using our open loop algorithm. This error (6nm RMS) is very close to the measurement floor (5 nm RMS of print-through and tilt).

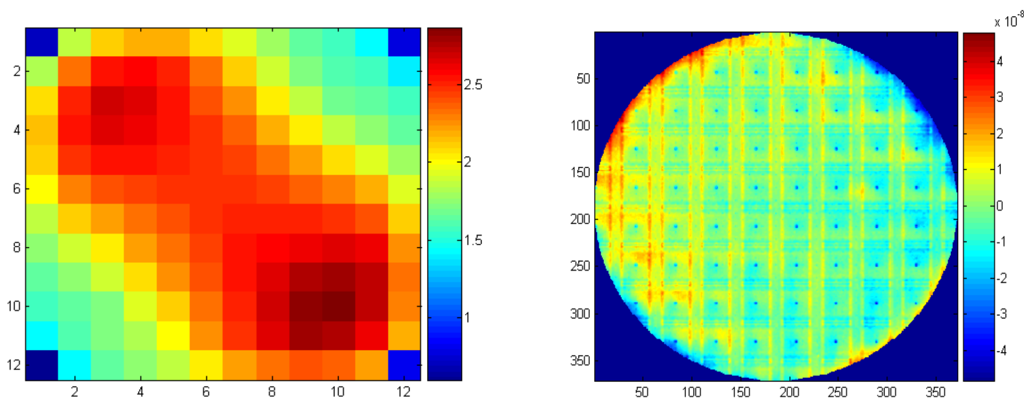

Figure 4: Open loop performance for a Zernike "Astigmatism" shape. Left- predicted deflections at posts. Right – open loop residual errors - **8.67nm RMS**.

Downloaded from SPIE Digital Library on 13 Mar 2010 to 24.218.156.200. Terms of Use: http://spiedl.org/terms

Results of other higher order Zernike shapes with peak-to-valley deflections up to 1.5 µm deflections are shown in the table below.

Table 1: RMS error results for the evaluation of the open-loop control algorithm using Zernike shapes on 12x12 DM.

Zernike Shape	Peak-to-valley deflection (µm)	RMS error (nm)
Astigmatism	0.5	8.3
	1.0	8.7
	1.5	17.1
Positive Focus	0.5	11.7
	1.0	17.6
	1.5	27.8
Trefoil	0.5	15.2
	1.0	18.2
	1.5	23.3
Coma	0.5	11.5
	1.0	19.3
	1.5	28.6

4. Conclusion

Previous open-loop control algorithm were demonstrated using a differential method, where the shapes tested were first imparted on the DM. Improvements in measurement filtering, calibration method, and accounting for the DM initial shape allowed us to control the true, non-differential desired shape with high accuracy over wider variety of deflection profiles including flattening and Zernike polynomials. Direct measurements of Zernike shapes with large deflection amplitudes in the order of 1.5 µm have been achieved with better than 30 nm accuracy. Low deflection amplitudes (500nm or less) resulted in less than 15 nm RMS error.

References

[1] Stewart, J.,B., Diouf, A., Zhou, Y., Bifano, T.,G., "Open-loop control of a MEMS deformable mirror for large-amplitude wavefront control," Optical Society of America A 24(12), 3827-3833 (2007)

[2] Morzinski, K.,M., Harpsoe, K.,B.,W., Gavel, D., T., Ammons, S., M.,"The open-loop control of MEMS : Modeling and experimental results," Proc. SPIE 6467, (2007)

Downloaded from SPIE Digital Library on 13 Mar 2010 to 24.218.156.200. Terms of Use: http://spiedl.org/terms

[3] Vogel, C.,R., Yang, Q., "Modeling, simulation, and open-loop control of a continuous facesheet MEMS deformable mirror," Journal of the Optical Society of America a-Optics Image Science and Vision 23 (5), 1074-1081 (2006)

Downloaded from SPIE Digital Library on 13 Mar 2010 to 24.218.156.200. Terms of Use: http://spiedl.org/terms